

## Electron-Spin Paramagnetic Resonance Studies of Neutron-Irradiated LiF<sup>†</sup>

R. KAPLAN\*<sup>‡</sup> AND P. J. BRAY

*Department of Physics, Brown University, Providence, Rhode Island*

(Received 13 December 1961; revised manuscript received 27 November 1962)

The electron-spin resonance spectra of  $F$  centers in neutron-irradiated crystals of Li<sup>6</sup>F, Li<sup>7</sup>F, and LiF of normal isotopic content have been studied in order to test existing theories of  $F$ -center resonance absorption. The spectrum for Li<sup>6</sup>F has several interesting features and confirms the ENDOR measurements of Holton, Blum, and Slichter for crystals of normal isotopic content. Specimens of the latter composition have been subjected to a wide range of neutron doses in the present work and their spectra examined. For doses smaller than about  $10^{17}n/cm^2$  the spectra exhibit a resolved hyperfine structure on a Gaussian envelope. For doses exceeding  $10^{17}n/cm^2$ , changes are observed in resonance linewidth, shape, and spin-lattice relaxation time. The observations appear to be consistent with the view that the radiation-induced defects are not uniformly distributed in the crystals. Exchange interactions between paramagnetic defects in regions of high defect concentration appear to be responsible for the observed changes in the resonance spectra as the neutron dose is increased. Crystals which received doses in excess of  $10^{19}n/cm^2$  exhibit resonance absorption characteristic of conduction electrons in small particles of lithium metal. Annealing and saturation studies give some information regarding the spin-lattice relaxation of the conduction electrons in the metal particles.

### I. INTRODUCTION

THE electron-spin resonance (ESR) spectrum of irradiated single crystals of LiF contains a broad symmetric absorption band whose  $g$  value is close to the free electron value 2.00229. The problem of identification and characterization of this resonance has received much attention in recent years. Interest was spurred originally by the discovery by Lord<sup>1</sup> of a partially resolved hyperfine structure in the ESR spectrum of x-rayed LiF crystals. Lord explained his results by assuming that the hyperfine lines were due to  $F$  centers. Using the  $F$ -center model of Kip *et al.*<sup>2</sup> and assuming that the dominant hyperfine interaction of the  $F$ -center electrons was with the nuclear magnetic moments of the six surrounding nearest-neighbor lithium atoms, Lord predicted<sup>1</sup> a 19-line, isotropic ESR spectrum. Shortly after Lord's original work, investigations<sup>3-5</sup> by Kim, Kaplan, and Bray (KKB) showed that the hyperfine structure in x-rayed and neutron-irradiated crystals of LiF was strongly dependent on the crystal orientation in the applied magnetic field  $H$ , and that the number of hyperfine lines greatly exceeded 19 (see Fig. 1). Thus the observed hyperfine structure could not be consistent with the simple explanation originally proposed. It was suggested<sup>5</sup> by KKB that the major portion of the resonance absorption, namely a broad resonance envelope without resolved structure,

was due to  $F$  centers. The resolved structure was attributed<sup>5</sup> to another type of center, possibly an impurity center.

Subsequent work<sup>6-9</sup> by Holton, Blum, and Slichter, using electron-nuclear double resonance (ENDOR) and fast passage techniques as well as that of slow passage ESR employed by KKB, presented convincing arguments for the belief that the broad ESR near  $g=2$  in irradiated LiF is due exclusively to  $F$  centers. From ENDOR experiments Holton *et al.* obtained the hyperfine coupling constants for the first seven shells of atoms surrounding the  $F$ -center lattice site. Using the constants so obtained, they were able to reconstruct the ESR spectrum for several orientations of the crystal in the applied field  $H$ , obtaining good agreement with the observed spectra. In constructing the ESR spectra, Holton *et al.* considered separately only the first lithium and first fluorine shells surrounding the  $F$  center. The remaining shells were assumed merely to broaden the individual hyperfine lines to an extent calculated from a second moment formula of Van Vleck.<sup>10</sup> The most

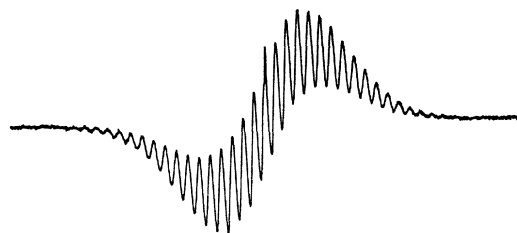


FIG. 1. ESR spectrum of a neutron-irradiated crystal of normal LiF with  $H$  along  $[111]$ . The neutron dose was  $10^{15} n/cm^2$ .

<sup>†</sup> Research supported by the U. S. Atomic Energy Commission under Contract AT(30-1)-2024.

\* Present address: U. S. Naval Research Laboratory, Washington, D. C.

<sup>‡</sup> Based on work performed by R. Kaplan in partial fulfillment of the requirements for the degree of Doctor of Philosophy at Brown University.

<sup>1</sup> N. W. Lord, Phys. Rev. **105**, 756 (1957).

<sup>2</sup> A. F. Kip, C. Kittel, R. A. Levy, and A. M. Portis, Phys. Rev. **91**, 1066 (1953).

<sup>3</sup> Y. W. Kim, R. Kaplan, and P. J. Bray, Bull. Am. Phys. Soc. **3**, 178 (1958).

<sup>4</sup> Y. W. Kim, R. Kaplan, and P. J. Bray, Bull. Am. Phys. Soc. **4**, 261 (1959).

<sup>5</sup> Y. W. Kim, R. Kaplan, and P. J. Bray, Phys. Rev. Letters **6**, 4 (1961).

<sup>6</sup> W. C. Holton, H. Blum, and C. P. Slichter, Phys. Rev. Letters **5**, 197 (1960).

<sup>7</sup> W. C. Holton, Ph.D. thesis, University of Illinois, 1960 (unpublished).

<sup>8</sup> H. Blum and W. C. Holton, Bull. Am. Phys. Soc. **6**, 112 (1961).

<sup>9</sup> W. C. Holton and H. Blum, Phys. Rev. **125**, 89 (1962).

<sup>10</sup> J. H. Van Vleck, Phys. Rev. **74**, 1168 (1948).

complete treatment of the work of Holton *et al.* is found in reference 9, which will be designated HB.

Further work by KKB on neutron-irradiated LiF has uncovered several areas where the observed behavior of the ESR spectra is not consistent with that expected from theories of the *F* center. One of these areas<sup>11</sup> deals with gradual but severe changes which occur in the ESR spectra as the neutron dose is increased over several orders of magnitude. A second is concerned with the saturation properties of the ESR spectra, which at first sight do not agree with Portis' theory of inhomogeneous broadening.<sup>12</sup> Some of the conclusions reached in the work on the second problem are in agreement with the results of recent investigations of neutron-irradiated LiF by Morigaki.<sup>13</sup>

In an effort to test the conclusions reached by Holton *et al.* concerning the *F*-center ESR spectrum in normal LiF, a study was made of the change in the spectrum to be expected if all of the lithium atoms were the isotope Li<sup>6</sup>. (Normal lithium is 93% Li<sup>7</sup>, 7% Li<sup>6</sup>.) It was found that, if the model and hyperfine coupling constants given in HB were correct, the *F*-center ESR spectrum of Li<sup>6</sup>F should show an unusually well-resolved hyperfine structure quite different from that observed from normal LiF. Following a description of experimental procedures in Sec. II of this paper, Sec. III contains a comparison of the predicted and observed *F*-center ESR in Li<sup>6</sup>F. Also included in Sec. III is a brief description of the ESR spectrum of a neutron-irradiated crystal of LiF in which 99.99% of the lithium nuclei are the isotope Li<sup>7</sup>.

In the remainder of the paper (Secs. IV-VI), a description is given of investigations of the ESR of neutron-irradiated LiF crystals of normal isotopic content. These crystals received doses in the range 10<sup>14</sup>-10<sup>20</sup> thermal neutrons per cm<sup>2</sup> (*n*/cm<sup>2</sup>). Over this range of dose a considerable variation in the dominant ESR absorption spectra was observed. In presenting and discussing these observations, it is convenient to distinguish three general types of resonance behavior associated with three ranges of neutron dose. Doses up to 10<sup>17</sup> *n*/cm<sup>2</sup> are called "light"; crystals which received light doses exhibit ESR spectra of the kind previously investigated by Lord,<sup>1</sup> KKB,<sup>3-5</sup> Holton *et al.*,<sup>6-9</sup> and others. The ESR spectra observed from LiF crystals in the light dose range are described and discussed in Sec. IV. Section V is concerned with crystals which received neutron doses in the "intermediate" range of 10<sup>17</sup>-10<sup>19</sup> *n*/cm<sup>2</sup>. In the intermediate range there is observed a strong dependence on neutron dose of resonance shape, width, and microwave power saturation. Certain crystals which received "heavy" doses, those in excess of 10<sup>19</sup> *n*/cm<sup>2</sup>, exhibit ESR lines charac-

teristic of conduction electrons in small particles of lithium metal, as described and discussed in Sec. VI.

The preceding limits set on the neutron dose ranges are somewhat arbitrary, since the effectiveness of a neutron dose in producing a particular kind of paramagnetic defect apparently depends on factors such as the crystal temperature during irradiation and on the concentrations of dislocations, vacancies, and other crystal defects in the unirradiated samples.

## II. EXPERIMENTAL PROCEDURES

The instrument used to obtain the ESR spectra was a Varian model V-4500 X-band spectrometer. This instrument yields recorder traces of the first derivatives of the absorption spectra. Unless noted otherwise, the spectra were run with the samples at room temperature.

Crystals of normal LiF were obtained from the following sources: Harshaw Chemical Company, Cleveland, Ohio; Optovac Company, North Brookfield, Massachusetts; Semi-Elements, Inc., Saxonburg, Pennsylvania; Dr. Karl Korth, Kiel, Germany. Each crystal was generally large enough to provide several dozen specimens, which were cleaved or cut from the large blanks. The specimens were in the shape of rectangular parallelepipeds with their long dimensions along either [100] or [110] crystalline axes. In the latter case the specimens could be rotated about their axes to bring a [111] direction parallel to the direction of the applied field *H*. Specimens of Li<sup>6</sup>F were obtained in a similar fashion from a blank grown in the laboratory by a method due to Stockbarger.<sup>14</sup> The starting material was polycrystalline Li<sup>6</sup>F enriched to 95.6% Li<sup>6</sup> and obtained from the Oak Ridge National Laboratory. A crystal of LiF enriched to 99.99% Li<sup>7</sup> was kindly supplied by Mr. Clay Weaver of the Reactor Division at the same laboratory.

Specimens were irradiated in the nuclear reactor of the Isotopes and Special Materials Division of the Brookhaven National Laboratory (BNL). Some specimens were annealed after irradiation in a regulated electric oven whose temperature was maintained and measured to about  $\pm 10^\circ\text{C}$ . The samples were enclosed in evacuated quartz tubes during annealing in those cases where contact of the atmosphere with the hot crystals was found to affect the results.

Measurement of the *g* values of *F*-center resonances was accomplished by observing simultaneously the ESR spectra of the LiF sample and of conduction electrons in a crystal containing small particles of lithium metal. Preparation of the latter sample will be described in Sec. VI. The technique is useful because the conduction electron resonance has a width no greater than 0.03 G and appears as a spike on the *F*-center spectra. (The observed width of 0.03 G must be considered an upper bound on the true linewidth, since the stability of the applied magnetic field of

<sup>11</sup> Y. W. Kim, R. Kaplan, and P. J. Bray, *Phys. Rev.* **117**, 740 (1960).

<sup>12</sup> A. M. Portis, *Phys. Rev.* **91**, 1071 (1953).

<sup>13</sup> K. Morigaki, *J. Phys. Soc. Japan* **16**, 1645 (1961).

<sup>14</sup> D. C. Stockbarger, *Rev. Sci. Instr.* **7**, 133 (1936).

approximately 3200 G was about one part in  $10^5$ .) Typical recorder traces of the conduction electron resonance superimposed on an  $F$ -center resonance are shown in Fig. 2 for normal LiF, (a), and  $\text{Li}^6\text{F}$ , (b). Measurements of the  $g$  shifts were made from traces having a smaller magnetic field scan rate than the traces of Fig. 2. The scan rate was measured with the aid of a nuclear magnetic resonance (NMR) proton gauss meter and an electronic frequency counter. Using the same equipment, the magnetic field strength at the center of the microwave cavity could be measured with the field adjusted to the conduction electron resonance value. The  $g$  value determined in this manner for conduction electrons in lithium metal is  $2.00229 \pm 0.00001$ , which is very close to the free electron value, as expected.<sup>15</sup> Measurement of the separation in magnetic field between the lithium conduction electron resonance and the centroid of the  $F$ -center hyperfine structure gives the  $F$ -center  $g$  values.

From the traces shown in Figs. 2(a) and 2(b), it is evident that the hyperfine patterns are shifted to lower values of the magnetic field than the conduction electron resonance and thus have measured  $g$  values higher than 2.00229. (As will be pointed out later, the measured  $g$  values must be corrected to take account of the presence of the hyperfine interaction.)

### III. ESR OF $F$ CENTERS IN $\text{Li}^6\text{F}$

#### A. Theoretical Spectrum

The formalism of HB has been followed in predicting the ESR absorption spectrum of  $F$  centers in  $\text{Li}^6\text{F}$ . Equation (8) of HB, which gives the frequencies at which absorption takes place, is

$$\begin{aligned} \Delta E_\alpha(M_i) = & g\beta_0 H_0 \\ & + [a_\alpha + b_\alpha(3 \cos^2\theta_\alpha - 1)]M_i(\text{shell}-1, \text{equiv.}) \\ & + [a_\alpha + b_\alpha(3 \cos^2\theta_\alpha - 1)]M_i(\text{shell}-2, \text{equiv.}), \end{aligned} \quad (1)$$

where the subscript  $\alpha$  identifies the nuclei in the ion shells surrounding the  $F$  center. The angle that the radius vector from the  $F$  center to the  $\alpha$ th nucleus makes with the direction of the applied field  $\mathbf{H}$  is designated  $\theta_\alpha$ . At the center of resonance,  $\mathbf{H}$  has the value  $\mathbf{H}_0$ . The quantity  $\beta_0$  is the Bohr magneton, and  $M_i$  is the  $z$  component of the total spin of each group of equivalent ions in shells 1 and 2. As pointed out by

TABLE I. Hyperfine coupling constants for  $\text{Li}^6$ ,  $\text{Li}^7$ , and  $\text{F}^{19}$  nuclei in shell-1 and shell-2 positions in LiF. Also given for each nuclear species are the nuclear spin  $I$ , and the magnetic moment  $\mu$  in multiples of  $\beta_N$ , the nuclear magneton.

Shell	Nucleus	$I$	$\mu$	$a$ (G)	$b$ (G)
1	$\text{Li}^7$	3/2	3.256	13.94	1.142
2	$\text{F}^{19}$	1/2	2.627	37.80	5.338
1	$\text{Li}^6$	1	0.822	5.279	0.432

<sup>15</sup> G. Feher and A. F. Kip, Phys. Rev. **98**, 337 (1955).

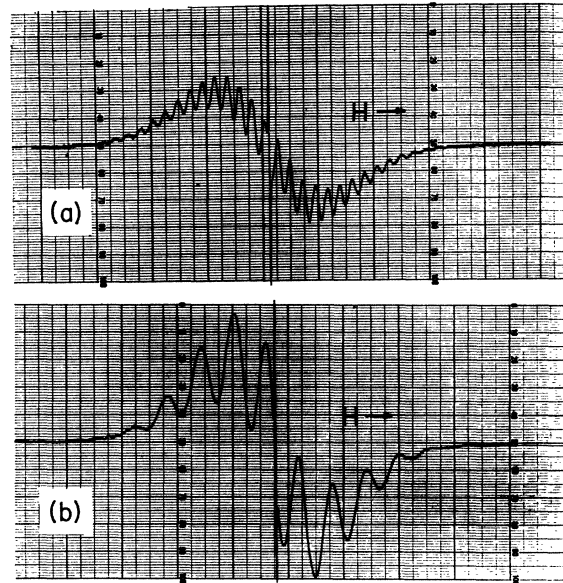


Fig. 2. Recorder traces similar to those used for evaluating the  $g$  shift of the  $F$ -center spectrum in normal LiF, (a), and  $\text{Li}^6\text{F}$ , (b). The sharp central line is due to conduction electrons in small particles of lithium metal observed simultaneously with the LiF crystals. The direction of increasing magnetic field scan is indicated by the arrows. The applied field  $\mathbf{H}$  is along  $[111]$  in (a), and  $[100]$  in (b).

Holton and Blum,<sup>9</sup> ions in a given shell may be non-equivalent either by having different values of  $\theta_\alpha$  for the particular orientation being considered, or by being different isotopes. Ions in shells beyond the second shell surrounding the  $F$ -center electron do not contribute resolved lines to the ESR spectrum because of the very low magnitude of their hyperfine coupling constants. These outer ions have the effect of broadening any resolved lines which arise due to hyperfine interactions with ions in the first and second shells. Again following HB,<sup>9</sup> the relative intensities of the transitions predicted by Eq. (1) are given by the relative statistical weights of the levels of different  $M_i$ .

The hyperfine coupling constants for the  $F$  center in normal LiF were determined by ENDOR experiments and given in HB; these constants are listed in Table I in units of magnetic field. Also included in Table I are the hyperfine coupling constants for  $\text{Li}^6$  nuclei in shell-1 positions. The latter constants are calculated from the  $\text{Li}^7$  shell-1 values on the basis of two assumptions. First, it is assumed that the  $F$ -center wave function is the same in  $\text{Li}^6\text{F}$  as it is in normal LiF. Second, it is assumed that the constants  $a_\alpha$  and  $b_\alpha$  are proportional to the quantities  $(\mu_\alpha/I_\alpha)$ . Then  $a_\alpha$  and  $b_\alpha$  may be adjusted to the nuclear magnetic moment  $\mu_\alpha$  and the nuclear spin  $I_\alpha$  of the isotope in question.

The ESR spectrum for  $\text{Li}^6\text{F}$  has been constructed for that orientation of the crystal which causes the applied field  $\mathbf{H}$  to be parallel to a  $[111]$  crystalline axis. This orientation causes the anisotropic terms in Eq. (1)

TABLE II. Statistical weights of the levels of  $M_i$  for the first shell  $\text{Li}^6$  nuclei,  $M_i^{(1)}$ , and the second shell  $\text{F}^{19}$  nuclei,  $M_i^{(2)}$  or  $M_i^{(2')}$ .

$M_i^{(1)}$	0	$\pm 1$	$\pm 2$	$\pm 3$	$\pm 4$	$\pm 5$	$\pm 6$
Weight	1.000	0.893	0.639	0.354	0.149	0.0425	0.0071
$M_i^{(2)}$ or $M_i^{(2')}$	0	$\pm 1$	$\pm 2$	$\pm 3$			
Weight	1.000	0.75	0.30	0.05			

to have a particularly simple form. For the first shell of lithium atoms,  $\cos\theta_\alpha$  is equal to  $1/\sqrt{3}$  for all six atoms, so that the factor multiplying  $b_\alpha$  is zero. For the second shell the lines joining each of six of the fluorine atoms to the  $F$ -center electron are perpendicular to  $\mathbf{H}$ , giving  $(3\cos^2\theta_\alpha - 1) = -1$  for these atoms. The other six fluorine atoms in the second shell have  $(3\cos^2\theta_\alpha - 1) = +1$  at this orientation. Thus the second shell divides into two groups of equivalent atoms, with six atoms in each group.

Equation (1) may now be rewritten in terms of the magnetic field amplitude  $H$  at which ESR absorption may occur. Hyperfine interactions involving shell-1  $\text{Li}^6$  nuclei are denoted by quantities bearing the superscript (1). The superscripts (2) and (2') identify shell-2  $\text{F}^{19}$  nuclei for which the quantity  $(3\cos^2\theta_\alpha - 1)$  has the values  $+1$  and  $-1$ , respectively. Using the constants listed in Table I, the result for  $H\parallel[111]$  is

$$\begin{aligned}
 H &= H_0 + a^{(1)} \sum_i m_i^{(1)} + (a^{(2)} + b^{(2)}) \sum_i m_i^{(2)} \\
 &\quad + (a^{(2')} - b^{(2')}) \sum_i m_i^{(2')} \\
 &= H_0 + 5.279 \sum_i m_i^{(1)} + 43.1 \sum_i m_i^{(2)} \\
 &\quad + 32.46 \sum_i m_i^{(2')}, \quad (2)
 \end{aligned}$$

where  $\sum_i m_i = M_i$  is the  $z$  component of the total spin of each group of equivalent ions. The quantities  $M_i$  can take integer values between the following limits:  $-6 \leq M_i^{(1)} \leq +6$ ;  $-3 \leq M_i^{(2)} \leq +3$ ;  $-3 \leq M_i^{(2')} \leq +3$ . A value of  $H$  occurs for every combination of values of  $M_i^{(1)}$ ,  $M_i^{(2)}$ , and  $M_i^{(2')}$ ; the latter three values occur independently of each other. The relative weight of a transition occurring at a particular value of  $H$  is the product of the weights of the three values of  $M_i$  in question. Altogether,  $13 \times 7 \times 7 = 637$  values of  $H$  are determined in this manner, forming an absorption spectrum symmetric about the value of  $H = H_0$ .

Equation (2) has been used to calculate the positions of all the hyperfine lines which occur at fields larger than  $H_0$ . The relative intensity of each hyperfine line was calculated as described above, using the weights given in Table II. The results of the calculation are given in Fig. 3 for the hyperfine line at  $H = H_0$  and the first 84 lines at higher magnetic fields. The remainder of the pattern is similar to the portion illustrated, except that the intensity of the spectrum drops off rapidly as

$H$  increases. The over-all spectrum is symmetric about the value  $H = H_0$ . Several features of the over-all spectrum may be noted. First, the hyperfine lines are segregated into ninety-seven groups, with each group containing between one and thirteen lines. Second, the spacing between the groups is quite uniform, averaging 5.4 G. Third, the most intense lines in each group are separated by between one-tenth and one gauss. Thus the spacing between groups is at least five times greater than the spread within each group. Fourth, the general decrease of intensity with increasing magnetic field is modulated by a periodic variation in the intensities of the individual groups. The period is equal to about seven group spacings.

On the basis of the foregoing analysis, it is possible to predict the appearance of the  $F$ -center ESR absorption spectrum that should be observed from a single crystal of  $\text{Li}^6\text{F}$  oriented so that  $\mathbf{H}\parallel[111]$ . The individual hyperfine lines are broadened by dipole-dipole interactions between  $F$ -center electrons<sup>16</sup> and by hyperfine interactions<sup>9</sup> with nuclei beyond the second shell of each  $F$  center. Since the widths attributable to these interactions are expected to be at least several tenths of one gauss, the individual hyperfine lines within each group should not be observable. Instead, the observed spectrum should consist of ninety-seven lines uniformly spaced by 5.4 G and arranged symmetrically about the central line. Each observed line then represents the envelope of a particular group of hyperfine lines. As discussed earlier, the number of hyperfine lines in a group varies from thirteen at the center of the spectrum to one at the ends. Since the individual hyperfine lines in each group are not expected to be resolved, the relative weight, or absorption intensity, of a given observed line should equal the sum of the weights of the hyperfine lines in the group in question.

The relative weights of the ninety-seven predicted absorption lines have been calculated from the weights of the individual hyperfine lines. In Fig. 4 the high-field side of the absorption spectrum is plotted schematically, with the relative intensities of the lines indicated by the

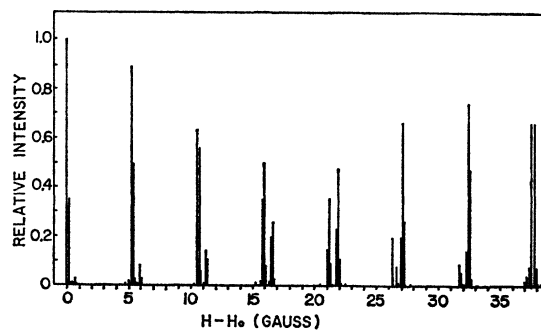


Fig. 3. Hyperfine lines predicted for the  $F$ -center ESR absorption spectrum in  $\text{Li}^6\text{F}$ . The central line and first 84 lines on the high-field side of the spectrum are shown.

<sup>16</sup> C. Kittel and E. Abrahams, *Phys. Rev.* **90**, 238 (1953).

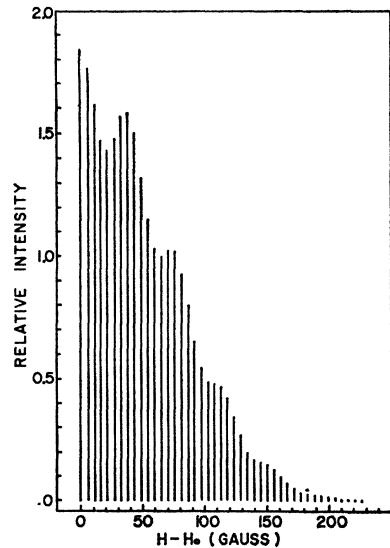


FIG. 4. Construction of the  $F$ -center hyperfine absorption spectrum that should be observable in  $\text{Li}^6\text{F}$  when  $\mathbf{H}$  is along  $[111]$ .

heights of the vertical bars. The foremost features of the complete spectrum are the following: (1) A total of ninety-seven equally spaced lines are present, with spacing equal to 5.4 G. (According to the predicted intensities, it is doubtful that the outermost few lines could be resolved.) (2) The intensity envelope of the ninety-seven lines displays thirteen peaks symmetrically arranged about the center of the spectrum. These peaks are separated by about seven spacings of the resolved lines, i.e., by about 37.8 G. Because of the scale of the spectrum of Fig. 4, only five of the six peaks on the high-field side of  $H_0$  are visible.

In most cases the ESR spectra of  $F$  centers exhibit no resolved structure, but instead appear as smooth absorption envelopes of approximately Gaussian shape. This situation exists because the many hyperfine lines which contribute to the spectra are not generally segregated into a relatively small number of groups; the separations between individual hyperfine lines are generally smaller than the widths of the lines. The reason that well-resolved structure may be observed in the ESR spectra of  $F$  centers in  $\text{Li}^6\text{F}$  becomes evident on examination of the hyperfine coupling constants of the nuclei in the first two shells surrounding the  $F$ -center electrons. The shell-2  $a$  value is equal to 7.16 times the shell-1  $a$  value, and to 7.1 times the shell-2  $b$  value. Because the coupling constants are very nearly integral multiples of each other, many of the hyperfine lines very nearly coincide, and segregation into groups of lines results. By placing the crystal in the external magnetic field so that  $\mathbf{H} \parallel [111]$ , the shell-1 anisotropic contribution to the ESR spectrum is eliminated. In any case, since the shell-1  $b$  value is less than 10% of the shell-1  $a$  value, little interference with the hyperfine resolution should be expected from the shell-1 anisotropic coupling at any angle.

Thus it is to be expected that the  $F$ -center spectrum

in  $\text{Li}^6\text{F}$  will show splittings related directly to the shell-1 and shell-2 isotropic hyperfine coupling constants. It might further be expected that by rotating the applied magnetic field direction away from a  $[111]$  crystalline axis, the smaller splittings due to the shell-1  $\text{Li}^6$  nuclei would be slightly mixed and smeared out, leaving the thirteen-line intensity envelope due to the shell-2  $\text{F}^{19}$  nuclei.

## B. Observed Spectrum

Electron-spin resonance spectra have been observed from two crystals of  $\text{Li}^6\text{F}$  which received neutron doses of  $5 \times 10^{13}$  and  $5 \times 10^{15}$   $n/\text{cm}^2$ , respectively. The former crystal was deep red in color after irradiation, the latter completely blackened. Resonance spectra from the two samples were the same except that the more heavily irradiated crystal gave resonance signals of greater intensity and poorer resolution than the more lightly irradiated sample. The latter sample was used in obtaining the spectra that are reproduced in the figures.

The observed spectra are shown in Fig. 5. Traces (a), (b), and (c) were obtained with the  $\text{Li}^6\text{F}$  crystal oriented so that  $\mathbf{H}$  was along  $[111]$ ,  $[100]$ , and  $[110]$  axes, respectively, of the sample. All of the traces were obtained with the same experimental arrangements. Measurements of the average splitting between lines gave the result  $5.6 \pm 0.4$  G. The periodic variation of envelope intensity is clearly visible in Fig. 5a; measurement gave the average separation of adjacent peaks of

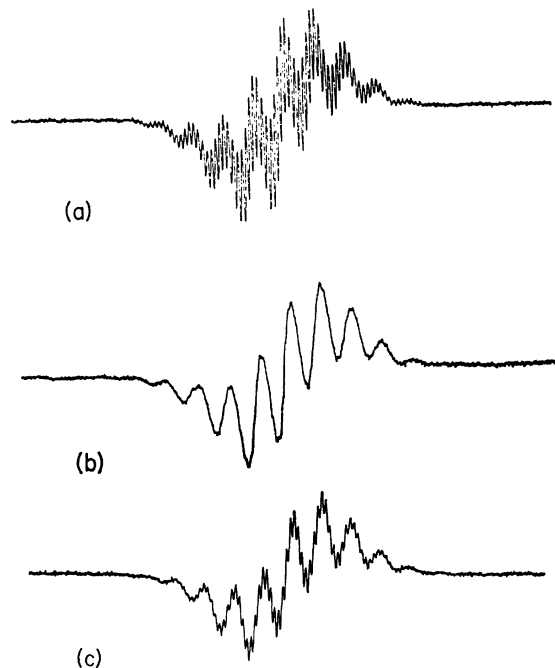


FIG. 5. ESR spectra observed for neutron-irradiated single crystals of  $\text{LiF}$ . (a)  $\text{Li}^6\text{F}$ ,  $\mathbf{H}$  along  $[111]$ . (b)  $\text{Li}^6\text{F}$ ,  $\mathbf{H}$  along  $[100]$ . (c)  $\text{Li}^6\text{F}$ ,  $\mathbf{H}$  along  $[110]$ . Scan rates in all traces are equal and are the same as that of the trace of Fig. 1.

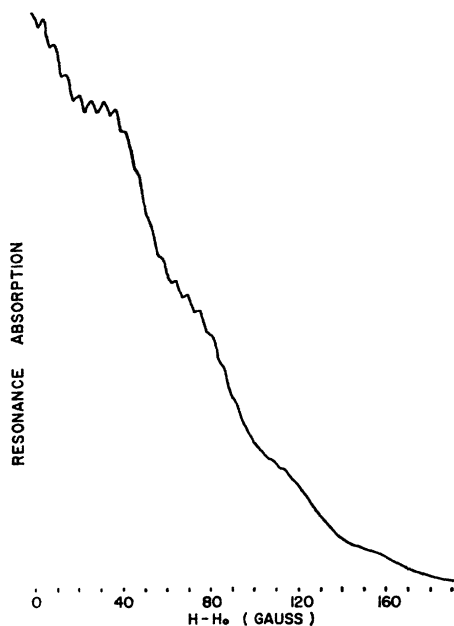


FIG. 6. Absorption spectrum (integrated recorder trace) of  $F$  centers in neutron-irradiated  $\text{Li}^6\text{F}$  with  $\mathbf{H}$  along  $[111]$ . Only the high-field half of the resonance is shown.

this variation as  $39.1 \pm 3.2$  G. About seventy resolved lines may be counted in the spectrum of Fig. 5(a). The number of absorption peaks in the spectrum whose derivative is shown in Fig. 5(b) is nine. Use of higher spectrometer gain reveals two further peaks on each side of this spectrum, although the outermost peaks are extremely weak. These ESR spectra may be compared with that of normal  $\text{LiF}$  (Fig. 1), which contains over thirty resolved lines equally spaced by 14.7 G and uniformly decreasing in intensity from the center of the spectrum toward the wings. This is the spectrum which has been interpreted in HB.

Since the hyperfine lines in the trace of Fig. 5(a) overlap somewhat, it is not possible to obtain directly a measure of the relative intensities of the lines. In order to compare the predicted and observed spectra directly, a recorder trace similar to that shown in Fig. 5(a) has been integrated graphically. (The trace used had a much slower scan rate to facilitate integration.) The result is shown in Fig. 6 for the high-field half of the absorption spectrum and is to be compared directly with Fig. 4. A quantitative comparison of the relative intensities of the predicted and observed hyperfine lines would entail development of theoretical line shapes and widths for the individual lines and summation over the entire spectrum. Qualitatively, however, the agreement between the predicted and observed spectra is evident.

It thus appears that the predicted and observed ESR spectra for  $F$  centers in  $\text{Li}^6\text{F}$  agree in all respects. From this agreement several conclusions may be drawn. First, the ESR spectrum of  $F$  centers in  $\text{LiF}$  is adequately described by Eq. (1). Second, the hyperfine coupling

constants for the first two ion shells in  $\text{LiF}$  are correct as given in HB. Third, the conclusion expressed in HB that the entire ESR spectrum of irradiated normal  $\text{LiF}$  is due to  $F$  centers is most probably correct. Important exceptions to the latter conclusion will be treated in following sections of the paper.

Normal  $\text{LiF}$  contains about 7% of the lithium isotope  $\text{Li}^6$ , the remainder being the isotope  $\text{Li}^7$ . The probability  $W(m)$  that the first shell of lithium atoms surrounding the  $F$ -center electron contains  $m$   $\text{Li}^6$  nuclei and  $(6-m)$   $\text{Li}^7$  nuclei may be calculated from the equation<sup>17</sup>

$$W(m) = \binom{6}{m} (0.93)^{6-m} (0.07)^m, \quad (3)$$

where the  $\binom{6}{m}$  are binomial coefficients. The probabilities for zero, one, and two  $\text{Li}^6$  nuclei appearing in the first shell are found from Eq. (3) to be 0.646, 0.292, and 0.055, respectively. Thus the number of  $F$  centers possessing one first-shell  $\text{Li}^6$  nucleus is nearly half of the number possessing all  $\text{Li}^7$  nuclei in the first shell. In order to determine how the  $\text{Li}^6$  nuclei present in  $\text{LiF}$  crystals of normal isotopic content affect the  $F$ -center hyperfine structure, experiments were performed on a single crystal of  $\text{LiF}$  enriched to 99.99%  $\text{Li}^7$  and irradiated in the BNL reactor. The hyperfine spectrum obtained from this sample was identical to that from crystals of normal isotopic content, except that the resolution of the hyperfine lines was somewhat improved. Thus the  $\text{Li}^6$  nuclei present in the normal  $\text{LiF}$  crystals do not affect such characteristics of the  $F$ -center spectra of these crystals as the number, spacing, and angular dependence of the resolved hyperfine lines.

The  $g$  values of the  $\text{Li}^6\text{F}$  and normal  $\text{LiF}$  spectra have been measured by the technique described in Sec. II. The results are: normal  $\text{LiF}$ ,  $g = 2.00303 \pm 0.00009$ ;  $\text{Li}^6\text{F}$ ,  $g = 2.00278 \pm 0.00006$ . The difference,  $g_{\text{meas}}(\text{normal LiF}) - g_{\text{meas}}(\text{Li}^6\text{F})$ , between these values is  $0.00025 \pm 0.00015$ . Since the  $F$ -center wave functions should not be sensitive<sup>18</sup> to the magnetic moments and spins of the neighboring nuclei, the  $g$  values of  $\text{Li}^6\text{F}$  and normal  $\text{LiF}$   $F$ -center spectra are expected to be equal.

A complicating factor is introduced by the need<sup>19</sup> for a second-order correction to the transition energy given by Eq. (1). This need arises because<sup>19</sup> the magnetic hyperfine interaction energy is not negligible compared to the Zeeman energy  $g\beta_0 H_0$ . The correction to the

<sup>17</sup> H. Margenau and G. M. Murphy, *Mathematics of Physics and Chemistry* (D. Van Nostrand Company, Inc., Princeton, New Jersey, 1957), p. 438.

<sup>18</sup> B. S. Gourary and F. J. Adrian, in *Solid State Physics*, edited by F. Seitz and D. Turnbull (Academic Press Inc., New York, 1960), Vol. 10, p. 127.

<sup>19</sup> G. Breit and I. I. Rabi, *Phys. Rev.* **38**, 2082 (1930).

measured  $g$  value may be obtained from the equation<sup>9</sup>

$$g_{\text{corr}} = g_{\text{meas}} \left\{ 1 - \left\langle \sum_{\alpha} \frac{1}{2} \left( \frac{a_{\alpha}'}{H_0} \right)^2 [I_{\alpha}(I_{\alpha}+1) - M_{\alpha}^2] \right\rangle \right\}, \quad (4)$$

where  $a_{\alpha}'$  is the effective coupling constant, including isotropic and anisotropic contributions, of the  $\alpha$ th nucleus which has spin  $I_{\alpha}$  and magnetic quantum number  $M_{\alpha}$ . In Eq. (4) the sum is over all nuclei which have appreciable values of  $a'$ ; i.e., over the first two shells in LiF. The summation is averaged over all possible combinations of all the nuclear spins, with each combination weighted according to its probability. Using this method, a correction of  $-0.0009$  is found in HB for normal LiF.

Rough calculations of the corrections to the  $g$  shifts in Li<sup>6</sup>F and Li<sup>7</sup>F have been made using Eq. (4). (The corrections for Li<sup>7</sup>F and normal LiF may differ slightly due to the fact that about three-tenths of the  $F$  centers in normal LiF possess one Li<sup>6</sup> nucleus in the first shell.) The calculations indicate that the magnitude of the correction for the Li<sup>7</sup>F spectrum is larger than that for the Li<sup>6</sup>F spectrum by 0.0004. Since the corrected  $g$  values should be equal, the relation  $g_{\text{meas}}(\text{normal LiF}) - g_{\text{meas}}(\text{Li}^6\text{F}) \cong 0.0004$  is predicted. As noted above, the observed value of this difference is  $0.00025 \pm 0.00015$ .

*Note added in proof.* A recent measurement by David L. Griscom of this laboratory has fixed the  $g$  value of Li<sup>7</sup>F to be  $2.00311 \pm 0.00008$ . This gives the difference  $g_{\text{meas}}(\text{Li}^7\text{F}) = 0.00033 \pm 0.00014$ .

#### IV. CRYSTALS IN THE LIGHT DOSE RANGE

##### A. Experimental Results

The ESR spectra of numerous LiF crystals which received neutron doses up to  $10^{17}$   $n/\text{cm}^2$  have been examined. These crystals, as well as all of those to be discussed in Secs. V and VI, contained the normal abundance of the isotopes Li<sup>6</sup> and Li<sup>7</sup>. Results of

TABLE III. Irradiation parameters for the LiF samples discussed in the text. Neutron fluxes and doses refer to thermal neutrons. Entries in the "Reactor Facility" column make use of the notation employed at BNL to identify the various positions in the reactor where specimens may be irradiated.

Sample number	Reactor facility	Neutron flux ( $n/\text{cm}^2 \text{ sec}$ )	Neutron dose ( $n/\text{cm}^2$ )	Estimated temperature of reactor facility ( $^{\circ}\text{C}$ )
1	w-13	$7 \times 10^{12}$	$1.3 \times 10^{16}$	75
2	w-13	$7 \times 10^{12}$	$3.5 \times 10^{14}$	75
3a	w-52	$5 \times 10^{12}$	$10^{16}$	30
4a	w-52	$5 \times 10^{12}$	$10^{17}$	30
5a	w-52	$5 \times 10^{12}$	$10^{18}$	30
6a	w-52	$5 \times 10^{12}$	$5 \times 10^{18}$	30
7a	w-52	$5 \times 10^{12}$	$5 \times 10^{18}$	30
7b	w-52	$5 \times 10^{12}$	$5 \times 10^{18}$	30
8a	w-13	$7 \times 10^{12}$	$10^{19}$	75
9	w-13	$7 \times 10^{12}$	$5 \times 10^{19}$	75

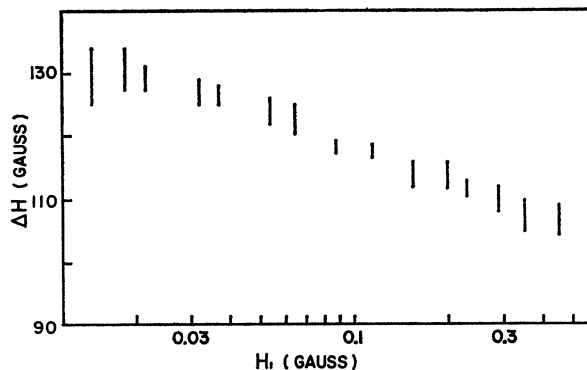


FIG. 7. Dependence of envelope width  $\Delta H$  on the microwave magnetic field amplitude  $H_1$ , for sample No. 1.

measurements on one of these crystals, designated sample No. 1, will be described in detail. In general, there is little variation among the spectra of crystals in the dose range  $10^{14}$ – $10^{17}$   $n/\text{cm}^2$  (aside from changes in resonance intensity), so that the measurements on sample No. 1 are typical of all those which have been made. Parameters describing the irradiation of all the samples to be discussed are collected in Table III. Measurements of the hyperfine structure were made with  $\mathbf{H}$  along  $[111]$ , whereas the crystals were oriented so as to avoid resolved structure when the envelope shape and width were observed.

Progressive saturation experiments were performed on the ESR of sample No. 1. Quantities observed as a function of the microwave magnetic field amplitude  $H_1$  were the width  $\Delta H$  of the resonance envelope between extrema of the derivative curve, the derivative intensity  $D|H - H_0|$  at a point removed from the center of resonance by  $|H - H_0|$ , and the derivative line shape.

The observed dependence of  $\Delta H$  on  $H_1$  is shown in Fig. 7. Over the range of available microwave power levels,  $\Delta H$  decreased as  $H_1$  was increased, from about 130 G at the lowest power level, to about 106 G at the highest. It appears that higher values of  $H_1$  would have yielded still smaller envelope widths. The situation at low-power levels is less clear because of the greater experimental uncertainty at these levels, but it is possible that smaller values of  $H_1$  would have yielded still wider resonance envelopes.

A second feature of the saturation data is the variation with  $H_1$  of the intensity  $D|\frac{1}{2}\Delta H|$  of the derivative peaks. According to Portis' theory of inhomogeneous broadening,<sup>12</sup>  $D|\frac{1}{2}\Delta H|/H_1$  should be proportional to  $(1+S)^{-1/2}$ , where the saturation parameter  $S = \gamma^2 H_1 T_1 T_2$ . Here  $T_1$  and  $T_2$  are the spin-lattice and spin-spin relaxation times, and  $\gamma$  relates the angular frequency and applied field at resonance:  $\omega_0 = \gamma H_0$ . However, it was not possible to fit the saturation data with a function of the form  $(1+S)^{-1/2}$ . A value of the quantity  $T_1 T_2$  chosen to fit the data at low microwave power levels predicted a more rapid decrease of derivative intensity at high

levels than was observed. The disagreement was only slightly lessened by measuring the derivative intensities a fixed distance of 65 G from  $H_0$ , in order to take account of the observed decrease in  $\Delta H$  under saturation.

The third quantity observed during saturation was the shape of the resonance envelope. At low microwave power levels the envelope shape was Gaussian, but a slight broadening was observed in the resonance wings at high power levels.

Observations of the hyperfine structure made with  $H$  along [111] showed that the decrease in  $\Delta H$  under saturation was not accompanied by change in the hyperfine spacing. As the microwave power level was raised, the resolution of the hyperfine structure gradually diminished, but the spacing remained constant.

After the measurements described above were completed, sample No. 1 was annealed for ten-minute periods at a succession of temperatures differing by 50°C. Observations of its ESR spectrum after each annealing period gave the following results. The envelope width and shape remained unaffected until the temperature exceeded 250°C. Heating at 300°C reduced  $\Delta H$  from 130 G to 85 G; further heating at 350°C yielded  $\Delta H=72$ G. The envelope changed abruptly from Gaussian to Lorentzian shape as a result of the annealing at 300°C and retained this shape until the resonance was destroyed by annealing at 400°C. A gradual decrease in resonance absorption intensity took place during the entire annealing process. In the interval between 250 and 300°C, where the envelope width and shape changed drastically, the number of paramagnetic centers contributing to the resonance was reduced by a factor of about two. Resolution of the hyperfine structure was reduced somewhat by the annealing, but the same hyperfine spacing and angular dependence were observed in the ESR spectrum before annealing and after the heating at 300 and 350°C. Finally, microwave power saturation experiments showed that the changes in envelope shape and width produced by annealing were accompanied by a decrease in the saturability of the resonance.

Measurements similar to those just described were made also on sample No. 2, which received a dose of  $3.5 \times 10^{14}$  n/cm<sup>2</sup> during a 50-sec exposure in the BNL reactor. (Sample No. 1 was irradiated in the same reactor facility for 30 min.) After irradiation sample No. 2 had a clear, light orange coloring. The results of the experiments on the two samples were qualitatively alike in all respects.

### B. Discussion

The data which have been presented lead immediately to the following conclusion: The observed ESR spectra are composite spectra representing absorption by more than one kind of paramagnetic center. The evidence for this conclusion is twofold. First, a single ESR line cannot be narrowed by saturation. If the resonance is

homogeneously broadened, it is expected<sup>12</sup> to widen at sufficiently high microwave power levels, while its shape and width should<sup>12</sup> not change if it is inhomogeneously broadened. Second, the hyperfine structure and envelope width and shape of a single inhomogeneously broadened resonance are uniquely related, so that one cannot change without change in the others. In the case of ESR spectra from unannealed samples, the same hyperfine structure was observed with envelopes as wide as 130 G and as narrow as 106 G. In the case of spectra from annealed samples, the same hyperfine structure was observed with envelopes of Lorentzian shape and widths as small as 72 G.

For convenience in the following discussion, it will be assumed that each of the composite resonances results from the superposition of two component resonances. One of the component resonances of each composite spectrum is the normal  $F$ -center resonance, which is characterized by its hyperfine structure and by an envelope width of about 150 G.<sup>6</sup> Some properties of the second component resonance may be deduced from the data described above. Changes in the composite spectra may be attributed both to changes in the relative strengths of the two components and to variation in the properties of the second component.

The second component evidently has a width smaller than 150 G; in the case of annealed samples it is as narrow as 72 G. Since the composite ESR line retains its symmetry in spite of changes produced by saturation or annealing, both component resonances must have symmetric envelopes and comparable  $g$  values. In particular, the  $g$  value of the second, or narrow component, is found to be isotropic. No resolved hyperfine structure characteristic of the narrow component is observed; the possibility that both resonance components have the same hyperfine structure has been ruled out by consideration of their widely differing envelope shapes and widths. Since the relative contribution of the narrow component to the composite spectrum is greater after annealing, when the saturability is decreased, the narrow component must be more difficult to saturate than the  $F$ -center component.

On the basis of this analysis, the decrease in  $\Delta H$  under saturation may be understood as arising from the greater relative contribution of the narrow component to the observed composite resonance at high microwave power levels. This explains the discrepancy between the values of  $\Delta H$  found for the  $F$  center in LiF by KKB,<sup>3-5</sup> on the one hand, and Holton *et al.*,<sup>6-9</sup> on the other. The latter workers used microwave power levels smaller than those available to the former. Thus the plot of  $\Delta H$  vs  $H_1$  in Fig. 7 would be expected to continue to rise as  $H_1$  was lowered beyond 0.01 G and to level off at a value of  $\Delta H \cong 150$  G.

The interpretation of the change in the observed resonance envelope width and shape during annealing is slightly more complicated, since there exist two possible explanations of this change. Annealing may

destroy  $F$  centers much more readily than the centers responsible for the narrow component, or it may convert some of the former centers to the latter. The observation that the drastic change in envelope shape and width between 250 and 300°C is accompanied by a decrease in the total number of paramagnetic centers by only a factor of about two, supports the second explanation. Since the composite spectrum still displays a strong hyperfine structure after the heating at 300°C, a substantial number of normal  $F$  centers remain in the sample at this stage of annealing. Graphical reconstructions of the composite spectra, similar to those to be described in the following section, indicate that a decrease in normal  $F$ -center concentration by a factor of two would not be sufficient to produce the observed change in envelope shape and width. This indicates that some conversion of the normal  $F$  centers to some other type of paramagnetic center must occur during annealing at temperatures above 250°C. Thus one result of the diffusion of paramagnetic centers induced by annealing is the formation of new centers, while another is the destruction of the original centers by recombination of lattice defects or by formation of nonmagnetic defects.

Thus the existence of a narrow component in the ESR spectrum of neutron-irradiated LiF has been demonstrated, and some of the properties of that component deduced from the results of saturation and annealing experiments. The narrow component is found in the spectra of crystals which received neutron doses as low as  $3.5 \times 10^{14}$   $n/cm^2$ , and had average  $F$ -center concentrations as small as  $10^{18}$   $cm^{-3}$ .

Two general questions concerning the narrow component resonances are yet to be answered. First, what centers are responsible for these resonances? Second, what are the experimental parameters, such as width and shape, that characterize the narrow components? It will be convenient to withhold discussion of these questions until data are presented, in the following section, for a series of crystals whose neutron doses span the light and intermediate dose ranges. The reason for this is that increasing the neutron dose beyond  $10^{17}$   $n/cm^2$  has a similar effect on the observed spectra as saturating or annealing more lightly irradiated crystals, in the sense that it increases the relative contributions of the narrow components to the composite spectra.

## V. CRYSTALS IN THE INTERMEDIATE DOSE RANGE

### A. Data

In examining the dependence of the ESR of irradiated LiF crystals on neutron dose, it is desirable to eliminate as far as possible effects due to dislocations and other crystal defects, sample preparation, environment during irradiation, and similar factors. Since their effects often are not distinguishable and cannot be eliminated, the factors mentioned must be controlled in such a way

that they affect similarly all samples whose ESR spectra are to be compared. Experiments were therefore performed on samples cut from a single large crystal blank, handled in identical fashion, and irradiated in the same reactor facility for different periods of time.

The experiments to be described were performed on five sets of samples fashioned and treated in the manner just described. The sets designated by the sample numbers 3, 4, and 5 received doses of  $10^{16}$ ,  $10^{17}$ , and  $10^{18}$   $n/cm^2$ . Sets No. 6 and No. 7 both received doses of  $5 \times 10^{18}$   $n/cm^2$  but were contained in separate packages during irradiation. Each set contained about five samples, whose ESR spectra were compared to check on the consistency of the results. One or more samples from each set were chosen for the measurements of resonance parameters which will be described.

It was not possible to obtain a neutron dose higher than  $5 \times 10^{18}$   $n/cm^2$  in the same reactor facility as that used for samples Nos. 3–7. For this reason the ESR spectra from the latter samples are compared with the resonance absorption by a specimen, designated No. 8, which received a dose of  $10^{19}$   $n/cm^2$  in a different reactor facility.

As will presently be described, variations were observed among the ESR spectra of crystals which were irradiated together and received neutron doses of  $5 \times 10^{18}$   $n/cm^2$  or more. This has prompted an investigation of the actual temperatures of the crystals during irradiation, since if the crystals were heated significantly by the thermal neutron reaction  $Li^6(n^1, He^4)H^3$ , their thermal contact with their surroundings in the reactor might be of decisive importance. In the first stage of these investigations, thermocouples were placed inside a large single crystal of LiF and in the free space inside the crystal's aluminum container, and the temperatures were measured during irradiation. Thermal contact between the crystal and container purposely was poor in this experiment, with only the edges of the crystal touching the metal container. The crystal temperature measured was about 200°C, whereas the air temperature inside the container at a point 1 in. from the crystal was found to be about 100°C. Since the samples used in the ESR experiments were considerably smaller than the crystal whose temperature during irradiation was measured, the former samples probably were not heated as strongly as the latter. Nevertheless, the ESR samples may have been heated sufficiently so that differences among their thermal contacts with their surrounding caused them to have different temperatures during irradiation. This might explain the variations observed among the ESR spectra of samples which received the same neutron dose in the same reactor facility. Further work on the effects of sample temperature during irradiation is in progress.

The results of studies of the ESR spectra of samples No. 3a, 4a, 5a, 6a, 7a, 7b, and 8a are now described. The observed variation of  $\Delta H$  with neutron dose is shown by the six recorder traces of Fig. 8. These traces

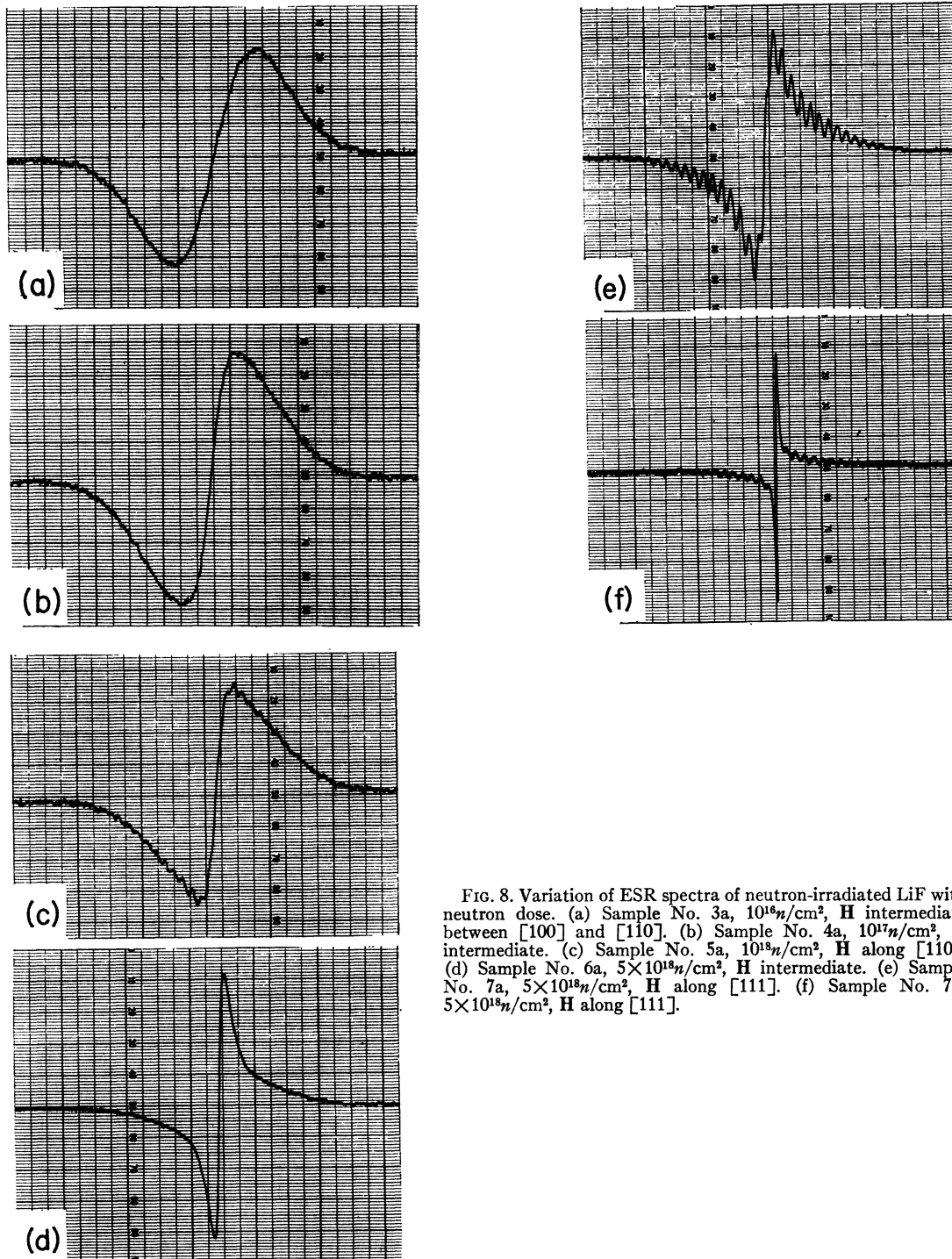


FIG. 8. Variation of ESR spectra of neutron-irradiated LiF with neutron dose. (a) Sample No. 3a,  $10^{16}n/cm^2$ ,  $H$  intermediate between  $[100]$  and  $[110]$ . (b) Sample No. 4a,  $10^{17}n/cm^2$ ,  $H$  intermediate. (c) Sample No. 5a,  $10^{18}n/cm^2$ ,  $H$  along  $[110]$ . (d) Sample No. 6a,  $5 \times 10^{18}n/cm^2$ ,  $H$  intermediate. (e) Sample No. 7a,  $5 \times 10^{18}n/cm^2$ ,  $H$  along  $[111]$ . (f) Sample No. 7b,  $5 \times 10^{18}n/cm^2$ ,  $H$  along  $[111]$ .

were obtained with equal magnetic field scan rates but different spectrometer gains. Traces (a), (b), and (c), representing the spectra of samples No. 3a, 4a, and 5a, show a monotonic decrease in  $\Delta H$  with dose, from 130 G at  $10^{16} n/cm^2$ , to 90 G at  $10^{17} n/cm^2$ , to 60 G at  $10^{18} n/cm^2$ . Trace (d) is the spectrum of sample No. 6a and

has  $\Delta H=19$  G. Two samples from the set designated No. 7 are represented by traces (e) and (f); the widths of these spectra are 35 and 4 G, respectively. The resonance of sample No. 8a is not shown in Fig. 8. Aside from having a width of 1.4 G, this resonance is qualitatively similar to the spectrum of sample No. 7b.

In general a smooth decrease of  $\Delta H$  with increasing dose is found for resonances wider than about 40 G, while an erratic dependence on dose appears for narrower lines. For the sets of samples which received doses of  $10^{16}$ ,  $10^{17}$ , and  $10^{18}$   $n/cm^2$ , the variation of resonance width among samples in a given set was less than 5%. Values of  $\Delta H$  for samples in the two sets which received doses of  $5 \times 10^{18}$   $n/cm^2$  ranged from 2 to 35 G.

The narrowing of the resonance lines with increasing neutron dose is accompanied by a gradual shift in line shape from Gaussian toward Lorentzian. However, spectra from crystals in the intermediate dose range often possess shapes which are neither Gaussian nor Lorentzian but rather appear to be superpositions of more than one resonance. Two such spectra are exhibited in Figs. 8(c) and 8(d). Regardless of their shapes, the resonances always appear symmetric about  $H_0$ .

The characteristic  $F$ -center hyperfine structure has been observed in the spectra of all crystals in the light and intermediate dose ranges. In spite of changes in envelope shape and width, the hyperfine spacing and angular dependence remain unaltered. In general, the hyperfine resolution becomes poorer as the neutron dose is increased.

That there is little change in the resonance  $g$  value as the neutron dose is increased may be deduced from the symmetry of the composite spectra that is observed for all values of  $\Delta H$ . In fact, a very slight shift of the measured  $g$  value towards the free-electron value occurs with increasing neutron dose. Thus the hyperfine structure in the spectrum of Fig. 8(e) is not oriented symmetrically with respect to the resonance envelope but is displaced to a lower magnetic field strength than the envelope, which therefore has the lower  $g$  value. The resonance illustrated in Fig. 8(f) is shifted to lower magnetic field strength than the lithium conduction electron resonance by 0.4 G, indicating a measured  $g$  value of  $2.00253 \pm 0.0002$ . This decrease from the value of 2.00303 measured for sample No. 3a reflects the decrease in the size of the second-order correction to the  $g$  value due to the weakening of the hyperfine interaction by exchange interactions.

The saturation properties of the observed resonances change as the neutron dose is increased. It is found that the saturability varies smoothly as a function of the observed linewidth, first decreasing and then increasing as the width decreases. In Table IV the effects of

TABLE IV. Saturation properties of the ESR spectra of six LiF samples. The quantities tabulated are the ratio of the value of  $\Delta H$  with  $H_1=0.45$  G to its value with  $H_1=0.01$  G, and the corresponding ratio for  $D|H-H_0|/H_1$  with  $|H-H_0|=\frac{1}{2}\Delta H$ .

Sample	3a	4a	5a	6a	7b	8a
$\Delta H$	135	90	60	19	4	1.4
$\Delta H(0.45)/\Delta H(0.01)$	0.74	0.61	0.85	1.0	1.0	1.0
$(D/H_1)(0.45)/(D/H_1)(0.01)$	0.15	0.45	0.7	1.0	0.85	0.8

saturation on the spectra of six samples are summarized. The quantities tabulated for each sample are the ratio of the value of the observed linewidth  $\Delta H$  in a microwave field of 0.45 G to its value in the field  $H_1=0.01$  G, and the corresponding ratio for  $D|\frac{1}{2}\Delta H|/H_1$ . The data show that the ratio  $(D/H_1)(0.45)/(D/H_1)(0.01)$  has a maximum for sample No. 6a, whereas the minimum of the ratio  $\Delta H(0.45)/\Delta H(0.01)$  occurs for sample No. 4a. The latter ratio depends not only on the widths of the component resonances producing the observed composite spectra but also on the relative intensities of the components. If the intensity of the narrow component compared to that of the normal  $F$ -center is very small, the observed width at low microwave power levels will be only slightly dependent on the narrow component. The decrease in width under saturation will then be large, as it is for sample No. 4a. The true measure of the saturability of the observed spectra is given by the dependence of  $(D/H_1)(0.45)/(D/H_1)(0.01)$  on  $H_1$ .

That the resonances of samples No. 3a, 4a, and 5a cannot be characterized by a single spin-lattice relaxation time  $T_1$  is evident from the fact that these resonances narrow under saturation. However, since the spectra of samples No. 6a, 7b, and 8a have Lorentzian shapes and do not narrow under saturation, it has been assumed that these spectra are homogeneously broadened and that they possess unique spin-lattice relaxation times. Analysis of the observed dependence of  $D|H-H_0|/H_1$  on  $H_1$  for samples No. 6a, 7b, and 8a has yielded the values of  $T_1$  and  $T_2$  given in Table V. (Other quantities appearing in Table V will be discussed later in this section.) The spin-spin relaxation time  $T_2$  is related to the resonance width  $\Delta H$  as follows<sup>20</sup>:  $T_2=2/(\gamma\sqrt{3}\Delta H)$ . Since no saturation of the resonance of sample No. 6a was observed, it was possible only to place an upper limit on  $T_1$  for this sample.

The theory of homogeneous broadening predicts<sup>12</sup> that the resonance width should be proportional to

TABLE V. Values of  $\Delta H$ ,  $T_1$ ,  $T_2$ , and  $\omega_e$  for the ESR spectra of six LiF samples.

Sample	3a	4a	5a	6a	7b	8a
$\Delta H$ (G)	80	55	50	19	4	1.4
$T_1$ (sec)	$10^{-6}$	$2.4 \times 10^{-6}$	$5 \times 10^{-6}$	$\leq 3.4 \times 10^{-7}$	$1.2 \times 10^{-7}$	$0.5 \times 10^{-7}$
$T_2$ (sec)	$8 \times 10^{-10}$	$1.2 \times 10^{-9}$	$1.3 \times 10^{-9}$	$3.4 \times 10^{-9}$	$1.63 \times 10^{-8}$	$0.44 \times 10^{-7}$
$\omega_e$ (kMc/sec)	5	7.2	7.8	21	99	260

<sup>20</sup> G. E. Pake, *Paramagnetic Resonance* (W. A. Benjamin, Inc., New York, 1962), p. 33.

$(1+S)^{1/2}$ . This quantity has been evaluated for the resonances of samples No. 7b and 8a, using plots of  $D|\frac{1}{2}\Delta H|/H_1$ . The results for a microwave field  $H_1=0.45$  G are: sample No. 7b,  $(1+S)^{1/2}=1.06$ ; sample No. 8a,  $(1+S)^{1/2}=1.07$ . Since the precision of the linewidth measurements is about 10%, increases in width by these amounts are not expected to be observable. As indicated in Table IV, the spectra of these samples were not observed to broaden under saturation.

Nuclear magnetic resonance (NMR) experiments have been performed on a number of crystals of neutron-irradiated LiF, including samples in the intermediate dose range. The latter samples always yielded  $\text{Li}^{7}$  NMR spectra characteristic of nuclei situated in an ionic lattice. The  $\text{F}^{19}$  NMR spectra showed, in addition to the usual broad resonance expected from ionic crystals, a sharp line which has been identified<sup>21,22</sup> as arising from fluorine gas formed during irradiation. The amount of gas formed and trapped in the crystals appears to depend<sup>22</sup> on the neutron dose and on other factors such as neutron flux and crystal temperature during irradiation. Sharp absorption lines have also been observed<sup>21,22</sup> in the  $\text{Li}^{7}$  NMR spectra of some LiF crystals which received heavy neutron doses. It will be shown in the following section that these lines are characteristic of small particles of lithium metal. As noted above, however, such lines were not observed in the  $\text{Li}^{7}$  NMR spectra of crystals in the intermediate dose range.

### B. Discussion

It was shown in Sec. IV that the ESR spectra of lightly irradiated LiF crystals are composite spectra, containing one or more components in addition to the normal  $F$ -center resonance. The arguments used in reaching this conclusion are equally valid when applied to the resonances of samples No. 3a, 4a, and 5a. As in the case of samples No. 1 and 2, the two major pieces of evidence are the following: (1) Although the over-all shapes and widths of the ESR spectra vary greatly with neutron dose, all of the spectra exhibit the same hyperfine structure spacing and angular dependence characteristic of the  $F$ -center resonance. (2) The resonance envelopes of the three samples in question are narrowed by microwave power saturation. The resonances of samples No. 6a, 7b, and 8a are also composite spectra, but here the difference in width between the  $F$  center and narrow components is sufficient for the latter components to be resolved and studied independently of the  $F$ -center absorption. This has been done with the results given in Table V.

The first of two general questions raised at the conclusion of Sec. IV concerns the origins of the narrow components in the LiF ESR spectra. Since it is known<sup>23</sup>

that many species of color center other than the  $F$  center are formed by irradiation at room temperature, the possibility that such centers are responsible for the narrow components must be considered. If such centers are the sources of the narrow components, the data might be explained by assuming that continued irradiation either would convert  $F$  centers into some other species or favor the production of the latter at the expense of further  $F$ -center production. However, several difficulties with this view are apparent. (1) In LiF irradiated at room temperature,  $M$  centers are the only color centers formed in quantities comparable to those of the  $F$  centers.<sup>23</sup> Resonance absorption by  $M$  centers has never been demonstrated unambiguously, and recent work<sup>24</sup> has indicated that  $M$  centers in LiF are not paramagnetic. Holton<sup>7</sup> also has found no effect of  $M$ -center concentration on the ESR spectra of irradiated LiF. Since in some LiF samples in the intermediate dose range the narrow component resonance intensity is comparable to that of the normal  $F$ -center resonance, it is unlikely that any of the well-known color centers are responsible for the ESR absorption. (2) In view of the great range of linewidths of the LiF ESR spectra, it would be necessary to assume that a number of different color centers, having a range of resonance widths, but equal  $g$  values, contribute to the composite spectra. The existence of such a distribution of centers is quite unlikely. (3) Unless a color center possesses spherical symmetry, its magnetic hyperfine interaction with neighboring nuclei will be strongly anisotropic. Examples of the anisotropy of spectra from centers not possessing such symmetry are provided by the  $V$  centers studied by Känzig and co-workers.<sup>25-28</sup> These spectra generally contain fairly small numbers of sharp, intense lines whose field positions depend strongly on the crystal orientation in the applied field. No such behavior on the part of the composite spectra in LiF is observed. Aside from the  $F$  center, the only color center that might possess spherical symmetry in LiF is the so-called "antimorph" of the  $F$  center, which may be described<sup>23</sup> as a positive hole trapped at a cation vacancy. However, Känzig has shown<sup>23</sup> that the electronic structure of this center does not possess spherical symmetry but rather resembles the structures of other  $V$  centers observed in LiF. In any event, the  $F$ -center antimorph is not stable at room temperature<sup>23</sup> and has a  $g$  value different from that of the  $F$  center.<sup>23</sup> Thus the isotropy, the lack of resolved structure, and the  $g$  value (equal to that of the  $F$ -center resonance) of the narrow component resonances are

<sup>24</sup> A. Okuda and K. Asai, Bull. Inst. Chem. Res. Kyoto Univ. 40, 81 (1962).

<sup>25</sup> T. G. Castner and W. Känzig, J. Phys. Chem. Solids 3, 178 (1957).

<sup>26</sup> T. O. Woodruff and W. Känzig, J. Phys. Chem. Solids 5, 268 (1958).

<sup>27</sup> M. H. Cohen, W. Känzig, and T. O. Woodruff, J. Phys. Chem. Solids 11, 120 (1959).

<sup>28</sup> W. Känzig, J. Phys. Chem. Solids 17, 80 (1960).

<sup>21</sup> P. J. Ring, J. G. O'Keefe, and P. J. Bray, Phys. Rev. Letters 1, 453 (1958); 2, 64 (1959).

<sup>22</sup> C. Knutson, H. O. Hooper, and P. J. Bray (to be published).

<sup>23</sup> F. Seitz, Rev. Mod. Phys. 26, 7 (1954).

not in agreement with the behavior expected from color centers other than  $F$  centers.

An alternative approach assumes that the narrow components are due to  $F$  centers in altered environments or to coagulated  $F$  centers. Inhomogeneously broadened resonance lines may be narrowed by rapid fluctuation of the surroundings of the electrons responsible for resonance absorption. This may occur by motion of the electrons, of the surrounding ions, or by exchange interactions between the electrons. Translational motion of ions or electrons in the ionic lattice may be ruled out for the following reasons: (1) Such motion would result in recombination of defects and disappearance of the ESR spectra. (2) The spectra are unaffected by cooling the samples to 78°K and to 4.2°K,<sup>13</sup> whereas lattice motion should be greatly reduced at these temperatures. (3) The narrow components are observed in crystals which received doses as small as  $3.5 \times 10^{14}$  n/cm<sup>2</sup> and do not contain regions of coagulated defects such as platelets of atoms<sup>29-32</sup> that might support ionic or electronic motion. (4) The narrow components display<sup>11</sup> an activation energy for thermal annealing that is characteristic of trapped-electron centers. (5) Finally, narrowing due to vibrational motion of lattice ions is ruled out by the observed temperature-independence of the linewidths, as noted in (2) above.

The possibility, previously suggested,<sup>11</sup> that the narrowed resonances are due to conduction electrons in small particles of lithium metal formed during irradiation may also be ruled out by several considerations. (1) The Li<sup>7</sup> NMR spectra of samples in the intermediate dose range contain no resonance lines due to lithium metal. Such lines have been observed from samples known to contain small metal particles, as noted previously. (2) The spin-spin and spin-lattice relaxation times of conduction electrons in metals are known<sup>15,33</sup> to be equal, due to the weakness of spin-spin interactions. However, only for sample No. 8a has equality of  $T_1$  and  $T_2$  been observed. (3) X-ray diffraction studies<sup>29-32</sup> of neutron-irradiated LiF have detected lithium metal particles in crystals which received doses in excess of  $10^{19}$  n/cm<sup>2</sup> but never in crystals which received smaller neutron doses. (4) Only the fraction ( $kT/E_F$ ) of conduction electrons in a metal will contribute to resonance absorption,<sup>20</sup> where  $E_F$  represents the Fermi energy of the metal. For lithium at room temperature ( $kT/E_F$ )  $\approx 0.01$ . Since the concentrations of electrons contributing to the narrow component resonances of such samples as No. 5a are of order  $10^{19}$  cm<sup>-3</sup>, these samples would have to contain about  $10^{21}$  metal atoms per cm<sup>3</sup> if the resonances in

question were due to conduction electrons. This represents about 1/60 of the lithium atoms in the crystals, which is a very large amount considering the facts that (i) these crystals remain intact and retain their cleavage properties after receiving neutron doses which produce the concentrations of centers in question, and (ii) x-ray<sup>29-32</sup> and NMR<sup>21,22</sup> experiments fail to detect lithium metal in these samples.

The remaining mechanism which would yield narrow resonance lines is the exchange interaction between trapped electrons. This possibility was discussed briefly by Morigaki.<sup>13</sup> The effects of exchange narrowing on ESR spectra have been considered by several authors, with particular emphasis being placed on changes in resonance shape and width<sup>10,34,35</sup> and spin-lattice relaxation time.<sup>36</sup> An exchange-narrowed resonance is expected<sup>34,35</sup> to have a Lorentzian shape and a width  $\Delta H$  given by

$$\Delta H \approx \frac{\gamma \Delta H_p^2}{\omega_e} = \frac{\gamma \Delta H_p^2}{J/\hbar} \quad (5)$$

in cases of strong narrowing, i.e., when  $\gamma \Delta H_p \ll \omega_e$ . In Eq. (5),  $\Delta H_p$  is the linewidth in the absence of narrowing, and  $J$  is the exchange integral, which may be written in terms of a rate  $\omega_e$  of spin exchange:  $J = \hbar \omega_e$ . When  $\gamma \Delta H_p \gg \omega_e$ , the line shape and width are unaffected by the exchange interaction. Anderson<sup>34</sup> has calculated the dependence of  $\Delta H$  on the ratio  $\gamma \Delta H_p / \omega_e$  in the intermediate case, where  $\gamma \Delta H_p \approx \omega_e$ . The saturation properties of exchange-narrowed resonances have been examined by Bloembergen and Wang, who found<sup>36</sup> that the exchange interaction provided a strong relaxation mechanism, thereby shortening  $T_1$ . Saturation of exchange-narrowed ESR lines was described by the formalism of homogeneous broadening, using appropriate values of  $T_1$ .

All of the measurements on the narrow ESR components in the LiF spectra, such as variations in linewidth and shape, relaxation,  $g$  value, resonance symmetry, and isotropy, can be explained qualitatively on the basis of a model of exchange interactions between  $F$  centers. On the other hand, alternative explanations of the data, as discussed above, appear unsatisfactory. An attempt has been made, therefore, to treat the data in as quantitative a fashion as possible, on the basis of a simple exchange-narrowing model. A description of this model follows.

It is assumed that the ESR spectrum of each irradiated LiF crystal contains two resonance components. One of these is the normal  $F$ -center resonance, whose envelope is Gaussian and 150 G wide. The other component is an exchange-narrowed  $F$ -center spectrum which originates in regions in the crystal where the

<sup>29</sup> M. Lambert and A. Guinier, *Compt. Rend.* **244**, 2791 (1956).

<sup>30</sup> M. Lambert and A. Guinier, *Compt. Rend.* **245**, 526 (1957).

<sup>31</sup> M. Lambert and A. Guinier, *Compt. Rend.* **246**, 1678 (1958).

<sup>32</sup> M. Lambert, Ph.D. thesis, University of Paris, 1958 (unpublished).

<sup>33</sup> A. W. Overhauser, *Phys. Rev.* **89**, 689 (1953).

<sup>34</sup> P. W. Anderson, *J. Phys. Soc. Japan* **9**, 316 (1954).

<sup>35</sup> P. W. Anderson and P. R. Weiss, *Rev. Mod. Phys.* **25**, 269 (1953).

<sup>36</sup> N. Bloembergen and S. Wang, *Phys. Rev.* **93**, 72 (1954).

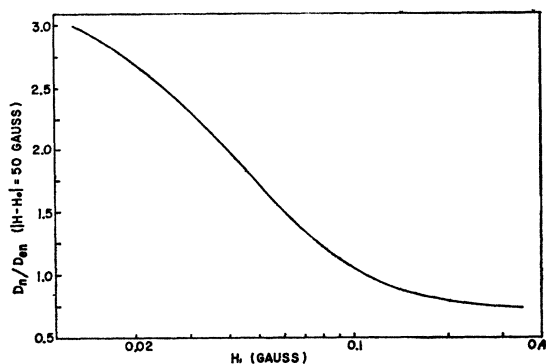


FIG. 9. Reconstruction of the ESR spectrum of sample No. 3a, according to the exchange-narrowing model. The ratio of the derivative intensity of the normal  $F$ -center component,  $D_n|H-H_0|$ , to that of the exchange narrowed component,  $D_{en}|H-H_0|$ , is shown as a function of  $H_1$ .

$F$ -center concentration is abnormally high. The narrowed component has an envelope of Lorentzian shape and width less than 150 G and a value of  $T_1$  smaller than the corresponding  $F$ -center relaxation time. The analysis consists in fitting the observed resonance line shape, linewidth, and microwave field dependence of  $\Delta H$  and  $D|H-H_0|$  by forming a composite resonance line from two envelopes, one a Gaussian 150 G wide and the other narrower and Lorentzian. The spin-lattice relaxation time of the Gaussian component is determined by fitting the observed dependence of  $D|H-H_0|$  on  $H_1$  at low microwave power levels. The width of the Lorentzian component is estimated from the observed envelope width at high-power level. Sets of composite resonances are then constructed graphically from pairs of superposed resonance derivative lines drawn with the appropriate shapes and widths. The value of  $T_1$  for the Lorentzian component and the relative intensities of the two components are determined by the requirement that the composite resonances reproduce the observed dependence of  $\Delta H$  on  $H_1$  and the observed line shape. The various resonance parameters finally are adjusted

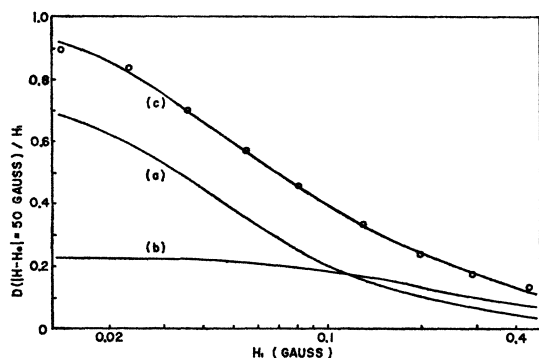


FIG. 10. Reconstruction of the ESR spectrum of sample No. 3a. (a) Saturation of the normal  $F$ -center component alone. (b) Saturation of the exchange-narrowed component alone. (c) Variation of the sum of curves (a) and (b) with  $H_1$ . The data points show the observed dependence of derivative intensity on  $H_1$ .

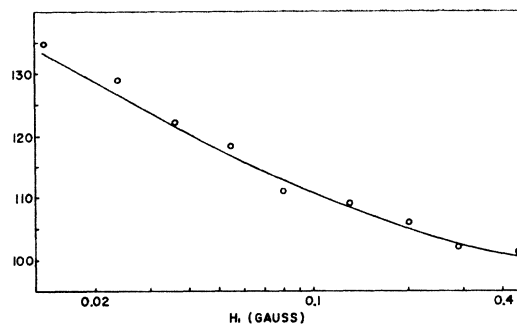


FIG. 11. Reconstruction of the ESR spectrum of sample No. 3a. The solid curve shows the dependence of the width of the theoretical composite resonance on  $H_1$ . The observed dependence on  $H_1$  is given by the data points.

to give the best possible fit to the data. It is found that the parameters are determined within a small range by this fitting process, which has been applied to the resonances of samples No. 3a, 4a, and 5a.

An example of the procedure is shown in Figs. 9–12, which give the results for sample No. 3a. The narrow component is assumed to have a width of 80 G and a value of  $T_1 = 10^{-5}$  sec, while the normal  $F$ -center component has  $T_1 = 2.5 \times 10^{-5}$  sec. This choice of relaxation times determines the variation with  $H_1$  of the relative intensities of the two components, after an initial ratio of intensities has been chosen. The result is shown in Fig. 9, in which  $D_n|H-H_0|$  represents the derivative intensity of the normal  $F$ -center component and  $D_{en}|H-H_0|$  that of the exchange-narrowed component. The same parameters determine the curves of Fig. 10, in which is shown the saturation of the  $F$ -center component alone, curve (a); of the narrow component alone, curve (b); and of the sum of these, curve (c). The data points represent the observed saturation of the composite resonance. The solid curve in Fig. 11 shows the decrease in width of the composite resonance under saturation, as given by the analysis. The observed decrease is given by the data points. Finally, the observed line shape at low microwave power is compared with that predicted by adding the two envelope components in Fig. 12.

A similar procedure has been followed in analyzing the ESR spectra of samples No. 4a and 5a, as noted above. This was not necessary in the case of samples No. 6a, 7b, and 8a, since for each of these samples the difference in width between the normal  $F$  center and exchange-narrowed components was sufficient for the latter to be studied directly, with the results given in Table V. Results for the narrow components of samples No. 3a–5a also are given in Table V.

The exchange frequency  $\omega_e$  was defined in Eq. (5) in terms of the widths  $\Delta H_p$  and  $\Delta H$  of the normal and exchange-narrowed  $F$ -center resonances. Equation (5) is valid in cases of strong narrowing. For the intermediate case when  $\gamma\Delta H_p \approx \omega_e$ , the relation between the quantity  $\Delta H/\Delta H_p$ , which is derived from the experi-

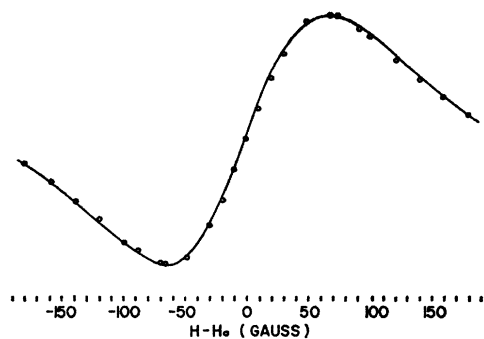


FIG. 12. Reconstruction of the ESR spectrum of sample No. 3a. The theoretical composite line shape, indicated by the circles, is compared at a low microwave power level with the observed resonance, represented by the solid line.

ments and the ratio  $\gamma\Delta H_p/\omega_e$ , has been calculated by Anderson.<sup>34</sup> The results of this calculation are plotted in Fig. A-3 of reference 34. Using this figure and Eq. (5) in the appropriate cases, a value of  $\omega_e$  has been determined for each exchange-narrowed component resonance from the observed ratio  $\Delta H/\Delta H_p$ . Values of  $\omega_e$  are included in Table V.

The variation of relaxation time  $T_1$  with the quantity  $\gamma\Delta H_p/\omega_e$  is exhibited in Fig. 13, as derived from the analysis using the exchange-narrowing model. By virtue of its definition as linewidth parameter,  $T_2$  varies inversely with  $\gamma\Delta H_p/\omega_e$ . The expected decrease of  $T_1$  with increasing strength of the exchange interaction is observed, as indicated in Fig. 13. For sample No. 8, which has  $\gamma\Delta H_p/\omega_e=0.01$ ,  $T_1$  and  $T_2$  are approximately equal. This is the situation to be expected<sup>36</sup> for extreme exchange narrowing; the exchange energy modulates the dipolar interaction, and magnetic energy is converted into exchange energy with a relaxation time  $T_1$  about equal to  $T_2$ . It should be noted that  $T_1$  in such a situation is actually a spin-spin relaxation time, though the relaxation process is similar to spin-lattice relaxation in that magnetic energy is not conserved.<sup>36</sup>

The composite resonance model described above was presented with the aim of adding to the plausibility of the interpretation of the observed spectra based on exchange narrowing between  $F$  centers. As noted above, the data are in agreement with the idea of exchange narrowing, whereas other possible explanations are beset with various difficulties. The exchange-narrowing model implies the existence of a highly nonuniform distribution of  $F$  centers in the irradiated crystals. The existence of such a distribution may not be surprising in view of the known<sup>37</sup> tendency of high quality alkali halide crystals to contain extensive regions in which the vacancy concentrations are some 100 times higher than in the bulk of the lattice.

Experiments similar to those which have been described have been performed on crystals of NaCl which

<sup>37</sup> O. Theimer and C. A. Plint, *Ann. Phys. (N. Y.)* **3**, 408 (1958).

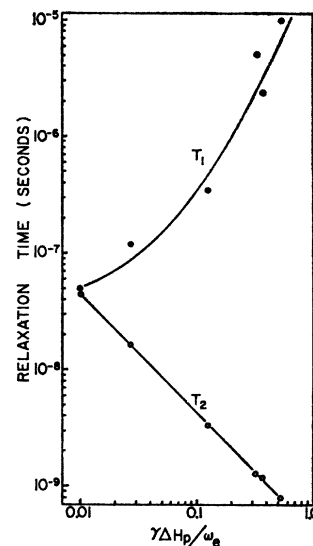


FIG. 13. Variation of  $T_1$  and  $T_2$  with  $\gamma\Delta H_p/\omega_e$  for six LiF samples, according to the exchange-narrowing model. The value of  $T_1$  at  $\gamma\Delta H_p/\omega_e=0.125$  is an upper limit for sample No. 6a, as explained in the text. The order of the samples represented by the data points is as follows, from right to left along the horizontal axis: 3a, 4a, 5a, 6a, 7b, 8a.

received doses of about  $10^{19}$  fast neutrons per square centimeter at BNL. The widths of the ESR spectra of these samples were found to decrease sharply under saturation, in a manner similar to that described for LiF crystals. Thus the spectra in NaCl samples also appear to be composite spectra possessing narrow and broad components, with the former having the shorter values of  $T_1$ . These observations indicate that the composite ESR spectra are not peculiar to radiation-damaged LiF. In addition, since nuclear fission does not occur in NaCl crystals during irradiation, it appears that the fission process is not required to produce the damage which yields the composite ESR spectra.

## VI. CRYSTALS IN THE HEAVY DOSE RANGE

### A. Experimental Results

Some crystals which received doses of about  $10^{20}$   $n/cm^2$  acquired a colorful metallic sheen quite unlike the dull black of other heavily irradiated crystals. Samples with the metallic appearance gave narrow, Lorentzian ESR spectra which, unlike the resonances of the samples previously described, did not disappear when the crystals were heated to about  $450^\circ C$ . In addition, crystals having the metallic sheen could not be decolorized at temperatures as high as  $730^\circ C$ ; they acquired instead a milky white appearance. All other irradiated LiF crystals regained their initial colorless, transparent state when heated to about  $500^\circ C$ .

The narrow ESR spectra from the samples which had the metallic appearance after irradiation were previously<sup>11</sup> identified as being due to conduction electrons in particles of lithium metal. Some of the observations which support this identification are the following.

- (1) The ESR spectra are not destroyed by annealing, as are those of color centers formed by irradiation.
- (2) The  $g$  value is  $2.00229 \pm 0.00001$ , which is extremely

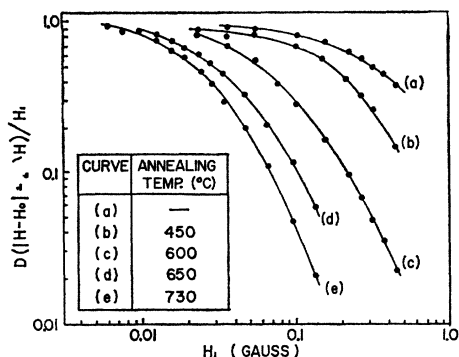


FIG. 14. Saturation of the ESR spectrum of sample No. 9 as a function of the temperature at which the sample was annealed.

close to the free electron value, as expected.<sup>15</sup> (3) The relation  $T_1 \cong T_2$  is satisfied, as determined by linewidth and saturation measurements. (4) Measurements of the  $\text{Li}^{7}$  NMR spectra of the samples in question reveal a sharp absorption line whose frequency shift is equal to the Knight shift of the resonance of  $\text{Li}^{7}$  nuclei in lithium metal. The width of the sharp line appears to be due to the inhomogeneity of the applied magnetic field when the sample is observed at room temperature. When the sample is cooled with dry ice to about  $-78^\circ\text{C}$  the sharp line is greatly broadened. These characteristics clearly identify the sharp  $\text{Li}^{7}$  resonance as being due to nuclei in lithium metal. The narrowness of the resonance at room temperature is due to self-diffusion of the lithium atoms in the metal.<sup>38</sup>

A number of extensive changes occur in the ESR spectra of the metal particles as the host crystals are annealed. Measurements on a typical crystal, sample No. 9, are described. The ESR line shape of sample No. 9 remains Lorentzian throughout the annealing process, but the width drops from about half a gauss before annealing, to 0.03 G after heating for 30 min at  $730^\circ\text{C}$ . The value 0.03 G must be considered an upper bound, since it is comparable to the limit of stability of the applied magnetic field. Accompanying the decrease in width by a factor of about 17 was an increase in the derivative intensity  $D|\frac{1}{2}\Delta H|$  by about 100 times. Integration of the recorder traces yields the resonance absorption spectra, and a second integration gives the area under each absorption curve. The area is proportional<sup>39</sup> to the number of electrons contributing to the resonance, and also to the quantity  $(\Delta H)^2 D|\frac{1}{2}\Delta H|$  measured on the derivative traces. From the values given above for  $\Delta H$  and  $D|\frac{1}{2}\Delta H|$ , it is evident that the transformation due to annealing caused the number of conduction electrons, or the total volume of metal, to be reduced to about one third of its initial value.

Since the variation of  $\Delta H$  with increasing annealing

<sup>38</sup> H. S. Gutowsky and B. R. McGarvey, *J. Chem. Phys.* **20**, 1472 (1952).

<sup>39</sup> D. J. E. Ingram, *Free Radicals as Studied by Electron Spin Resonance* (Butterworths Scientific Publications, London, 1958), p. 34.

TABLE VI. Measured values of  $T_1$  and  $T_2$  for sample No. 9 at various stages of annealing.

Annealing temp. (°C)	*	450	600	650	730
$T_2$ (sec $\times 10^7$ )	1.3	2.1	7.3	12	22
$T_1$ (sec $\times 10^7$ )	1.3	2	5	11	14

\* Unannealed sample.

temperature is a smooth variation, it is unlikely that a sudden conversion from coagulated  $F$  centers or other defects to metal particles occurs. That is, the sharp resonances observed before annealing, as well as those observed after heating the sample, are due to conduction electrons. The existence of metal particles in the unannealed samples is demonstrated by NMR and x-ray diffraction experiments, as discussed earlier.

Another change produced by annealing is an increase in spin-lattice relaxation time  $T_1$ . Saturation curves for the resonance of sample No. 9 are shown in Fig. 14. Curve (a) represents the unannealed sample, and the other curves represent various stages of annealing. Values of  $T_1$  have been extracted from these curves and compared with the values of  $T_2$  obtained from the linewidth at each stage of annealing. Within a factor of two, the spin-spin and spin-lattice relaxation times are found to be equal after each change produced by annealing. The values of  $T_1$  before annealing and after heating at  $730^\circ\text{C}$  for 30 min were  $1\times 10^{-7}$  sec and  $14\times 10^{-7}$  sec, respectively. The values measured at each stage of annealing are given in Table VI.

The ESR line of sample No. 9 retained its symmetry throughout the annealing process with the exception of the last treatment at  $730^\circ\text{C}$ . After this treatment the spectrum was asymmetric when the sample was observed while cooled with liquid nitrogen but regained its Lorentzian shape when the crystal was warmed to room temperature. This is the behavior expected<sup>15,40</sup> for metal particles whose dimensions are comparable to the skin depth of the microwave field in the metal at the temperature of liquid nitrogen.

## B. Discussion

It is of interest to determine the mechanism responsible for the spin-lattice relaxation, and hence the linewidth, of the conduction electron resonances. Unfortunately, the two plausible mechanisms, impurity scattering and scattering by the surfaces of the metal particles, are hard to distinguish from each other. The lengthening of  $T_1$  during annealing might reflect either growth or purification of the particles.

A rough estimate of the particle size after heating at  $730^\circ\text{C}$  may be achieved by assuming that the particles are spherical and that their diameters are equal to the skin depth of the microwave field in lithium at  $78^\circ\text{K}$ . This estimate yields a diameter of  $0.6\ \mu$ . Assuming that

<sup>40</sup> F. J. Dyson, *Phys. Rev.* **98**, 349 (1955).

the spin-lattice relaxation time depends only on surface relaxation throughout the annealing process, the linewidth may be expected<sup>15,40</sup> to vary inversely as the particle diameter. The linewidth for the unannealed sample was 0.5 G, and after the annealing at 730°, the width was 0.03 G. Thus the particle size in the unannealed sample, in this estimate, was about  $(0.03/0.5) \times 0.6 \mu$ , or roughly 360 Å. This value is in reasonable agreement with values of particle size determined by x-ray diffraction studies.<sup>31,32</sup>

Thus, it seems reasonable that the process which occurs during annealing of the host crystals is growth of the metal particles rather than purification of the metal in the particles. The increase in  $T_1$  and consequent decrease in linewidth would then be due to the lengthening of the time required by conduction electrons to reach the particle surfaces, as already described.

### VII. SUMMARY

Investigations of the ESR spectra of neutron-irradiated crystals of Li<sup>6</sup>F and Li<sup>7</sup>F have confirmed the *F*-center analysis by Holton *et al.*<sup>6-9</sup> of the resonance spectra of LiF crystals of normal isotopic content. The *F*-center spectrum in Li<sup>6</sup>F is unusual in that it possesses a hyperfine structure in which contributions from the first and second shells of neighboring nuclei may be individually identified.

Extensive changes occur in the ESR spectra of irradiated LiF crystals of normal isotopic content when the neutron dose is increased from about  $10^{14}$  n/cm<sup>2</sup> to over  $10^{20}$  n/cm<sup>2</sup>. For doses smaller than about  $10^{17}$  n/cm<sup>2</sup>, normal *F* centers are the predominant paramagnetic centers. The presence of narrower underlying spectra is revealed by saturation and annealing experiments. The underlying resonances appear to be due to *F* centers in certain regions of the crystals where the concentration of centers is great enough to permit the

occurrence of exchange narrowing with its accompanying decrease in the relaxation time  $T_1$ . For doses greater than about  $10^{17}$  n/cm<sup>2</sup>, the ESR spectra are narrowed and altered in shape, indicating an increase in the strength of the narrowed resonance components relative to that of the *F*-center components. This probably reflects a growth in the number or extent of the crystal regions containing high concentrations of *F* centers and growth of the concentrations themselves. The effect of thermal annealing on the lightly irradiated crystals is similar to that of further irradiation of these crystals in the sense that the proportion of centers contributing to the narrow resonance components is increased at the expense of the isolated *F* centers. This increase is believed to occur largely by the diffusion of *F* centers into regions of high *F*-center concentration during the time the crystals are heated.

Some crystals which received doses of about  $10^{20}$  n/cm<sup>2</sup> yielded ESR spectra characteristic of conduction electrons in small particles of lithium metal. The spectra were narrowed considerably when the crystals were annealed, lines as narrow as 0.03 G being recorded. The observed decrease in  $\Delta H$  and the accompanying increase in  $T_1$  are consistent with the view that spin-lattice relaxation occurs at the particle surfaces and that the particle size increases during annealing.

### ACKNOWLEDGMENTS

The authors wish to thank Alan C. Greene for furnishing and discussing the results of his measurements of crystal temperature during irradiation. The work of J. Deluisi in growing a single crystal of Li<sup>6</sup>F is greatly appreciated. Dr. R. A. Weeks of the Oak Ridge National Laboratory kindly aided the authors in obtaining a single crystal of Li<sup>7</sup>F. David L. Griscom has very graciously supplied the *g* values given for Li<sup>6</sup>F and Li<sup>7</sup>F and has contributed in other ways to this paper.

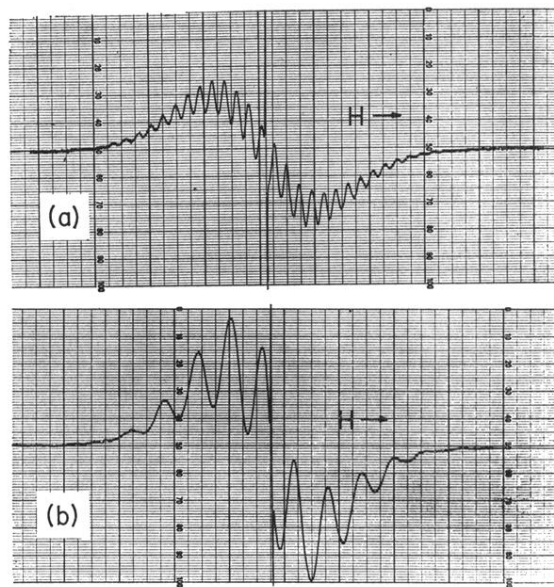


FIG. 2. Recorder traces similar to those used for evaluating the  $g$  shift of the  $F$ -center spectrum in normal LiF, (a), and  $\text{Li}^6\text{F}$ , (b). The sharp central line is due to conduction electrons in small particles of lithium metal observed simultaneously with the LiF crystals. The direction of increasing magnetic field scan is indicated by the arrows. The applied field  $\mathbf{H}$  is along  $[111]$  in (a), and  $[100]$  in (b).

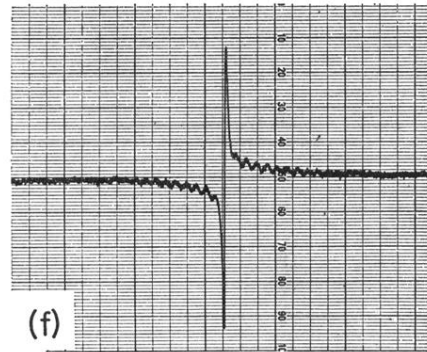
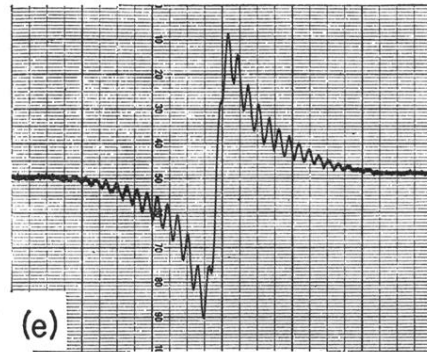
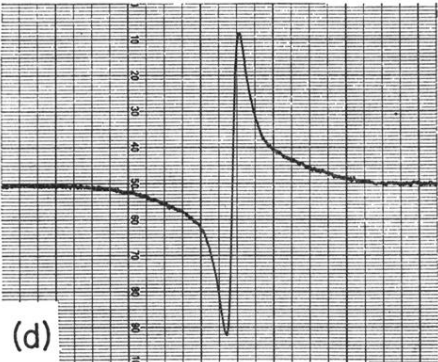
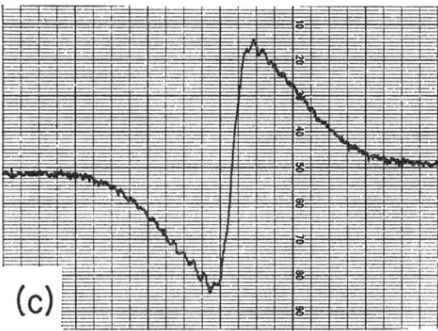
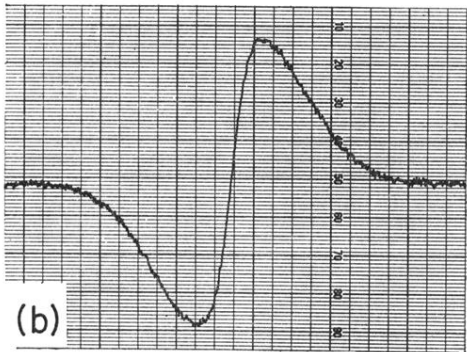
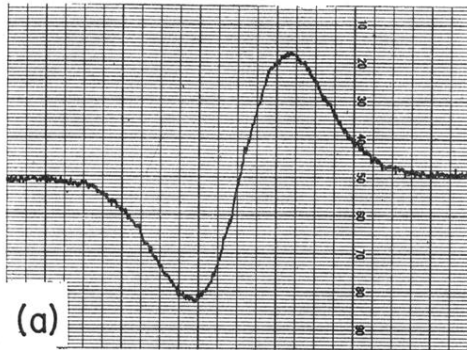


FIG. 8. Variation of ESR spectra of neutron-irradiated LiF with neutron dose. (a) Sample No. 3a,  $10^{16}n/cm^2$ , **H** intermediate between [100] and [110]. (b) Sample No. 4a,  $10^{17}n/cm^2$ , **H** intermediate. (c) Sample No. 5a,  $10^{18}n/cm^2$ , **H** along [110]. (d) Sample No. 6a,  $5 \times 10^{18}n/cm^2$ , **H** intermediate. (e) Sample No. 7a,  $5 \times 10^{18}n/cm^2$ , **H** along [111]. (f) Sample No. 7b,  $5 \times 10^{18}n/cm^2$ , **H** along [111].